

Polarizability of molecular clusters as calculated by a dipole interaction model

Lasse Jensen^{a)}

Theoretical Chemistry, Material Science Centre, Rijksuniversiteit Groningen, Nijenborgh 4, 9747 AG Groningen, The Netherlands

Per-Olof Åstrand

Materials Research Department, Risø National Laboratory, DK-4000 Roskilde, Denmark and Department of Chemistry, H. C. Ørsted Institute, University of Copenhagen, DK-2100 Copenhagen Ø, Denmark

Anders Osted, Jacob Kongsted, and Kurt V. Mikkelsen

Department of Chemistry, H. C. Ørsted Institute, University of Copenhagen, DK-2100 Copenhagen Ø, Denmark

(Received 20 June 2001; accepted 15 November 2001)

We have developed and investigated a dipole interaction model for calculating the polarizability of molecular clusters. The model has been parametrized from the frequency-dependent molecular polarizability as obtained from quantum chemical calculations for a series of 184 aliphatic, aromatic, and heterocyclic compounds. A damping of the interatomic interaction at short distances is introduced in such a way as to retain a traceless interaction tensor and a good description of the damping over a wide range of interatomic distances. By adopting atomic polarizabilities in addition to atom-type parameters describing the damping and the frequency dependence, respectively, the model is found to reproduce the molecular frequency-dependent polarizability tensor calculated with *ab initio* methods. A study of the polarizability of four dimers has been carried out: the hydrogen fluoride, methane, benzene, and urea dimers. We find in general good agreement between the model and the quantum chemical results over a wide range of intermolecular distances. To demonstrate the power of the model, the polarizability has been calculated for a linear chain of urea molecules with up to 300 molecules and one- and two-dimensional clusters of C₆₀ with up to 25 molecules. Substantial intermolecular contributions are found for the polarizability anisotropy, whereas the effects are small for the mean polarizability. For the mean polarizability of C₆₀, we find good agreement between the model and experiments both in the case of an isolated molecule and in a comparison of a planar cluster of 25 C₆₀ molecules with experimental results on thin films.
© 2002 American Institute of Physics. [DOI: 10.1063/1.1433747]

I. INTRODUCTION

The design of new carbon-based materials for potential use in optoelectronic and photonic devices is of great technological importance. These new materials will lead to a new generation of information technology where optical methods are the basis for rapid communication processes.¹⁻³ One promising class of materials is the so-called molecular materials, i.e., materials consisting of molecular entities. The optical response properties of this class of materials are to a large extent governed by the properties of the individual molecules and to some extent by the interactions with the neighboring molecules. Therefore, understanding the response properties of the bulk materials, the molecular response properties and the perturbations caused by environmental interactions are needed in order to achieve an efficient procedure for designing optical molecular materials at the atomistic level.^{1,4-9} From a theoretical point of view, the molecular response to an external electromagnetic field is

calculated most efficiently by applying quantum chemical response theory.¹⁰ Accurate quantum chemical calculations of molecular properties can, however, only be carried out for rather small molecules due to the large requirements of computer resources. Furthermore, the use of conventional density functional theory, which in general gives improved accuracy over the Hartree-Fock approximation at a similar or lower computational cost, gives relatively poor results for nonlinear optical properties of large conjugated molecular chains.^{11,12} Therefore, for large molecules and assemblies of molecules, modeling is currently restricted to less sophisticated methods.

The isotropic part of the molecular polarizability is to a good extent an additive property, indicating that the polarizability can be calculated from a sum of transferable atomic or bond contributions. However, perfect additivity can only occur if the subunits are noninteracting, which obviously is not the case for atoms in molecules. Therefore, as pointed out by Silberstein,¹³ the molecular polarizability is not additive unless the chemical environment of each atom is considered in detail. The chemical environment was first introduced by us

^{a)} Author to whom all correspondence should be addressed; electronic mail: l.jensen@chem.rug.nl

ing bond polarizability models,^{14,15} which were quite successful in reproducing the static mean polarizability (the isotropic part of the polarizability tensor) of alkanes.¹⁵ Different methods using the additivity concept have also been proposed^{16–18} and these models are in general successful in reproducing the molecular mean polarizability. Recently, the additivity model was adopted for the static polarizability tensors of organic molecules^{19,20} and also for both the static and frequency-dependent polarizability tensors of halogen derivatives of benzene²¹ using atomic polarizability tensor elements. However, since the molecular polarizability is a tensor, also the atomic contributions have to be tensors in an additive model leading to a larger number of parameters to be determined.

A more elaborate model, but yet very simple compared with quantum chemical calculations, is the dipole interaction model of Applequist *et al.*^{22–24} based on the early work of Silberstein.^{13,25,26} In the interaction model, the atoms of a molecule in an external field interact by means of their atomic induced dipole moments according to classical electrostatics. Even if the atomic parameters are isotropic polarizabilities, an anisotropy of the molecular polarizability is introduced by the electric fields from the surrounding atoms. An important extension of the interaction model was to include overlap effects on the internal electric fields,^{27–29} i.e., the electric field at the nucleus is damped. In particular, the model of Thole²⁸ has turned out to be successful in predicting the molecular polarizability tensor using model atomic polarizability parameters independent of the chemical environment of the atom. Thole's model has recently been investigated in more detail^{30–35} and also extended to include atom-type damping parameters and the treatment of the frequency-dependent polarizability tensor.^{34,35}

However, despite the success of the Thole model, a problem arises from the introduction of the damping term into the interaction tensor. The modification of the interaction tensor leads to a tensor which, in contrast to the undamped tensor, is not traceless. In addition, the most promising damping function suggested by Thole²⁸ is not continuous. This discontinuity may give problems at small intermolecular distances and is therefore not suitable for investigating intermolecular interactions.³³

In this study, we present a way of introducing a damping of the interaction tensor which preserves the traceless property of the interaction tensor. The formulas will in principle be valid for all terms of the interaction tensor in the multipole expansion. Furthermore, the way that atom-type damping parameters are introduced is given a more firm theoretical base than the more *ad hoc* approach adopted previously.

Both in the additivity and interaction models, the model atomic (or bond) polarizabilities are fitted to the molecular polarizabilities of a trial set of molecules. Therefore, the quality of the data in the trial set will affect the accuracy and the actual values of the model parameters. In particular, experimental molecular polarizabilities also include zero-point vibrational and pure vibrational contributions that most probably are not negligible.^{36–38} It is therefore preferred to use quantum chemical calculations of molecular electronic polarizabilities for the parametrization. Here, we extend the set of

aromatic and aliphatic molecules employed previously³⁴ to also include heteromonocyclic compounds containing B, N, and C atoms and we parametrize the model from *ab initio* frequency-dependent molecular polarizabilities. The obtained model will be used to study the interaction polarizability of four dimers, the HF, methane, benzene, and urea dimers. Since the aim of the work is to treat large molecular assemblies, we also present results for one-dimensional urea chains with up to 300 molecules and for one- and two-dimensional C₆₀ clusters with up to 25 molecules. To our knowledge, this is the first theoretical study of the polarizability of C₆₀ clusters and it gives the possibility of comparing with the polarizability obtained from experiment on thin films. The additional boron parameters are used in a separate work on boron nitride nanotubes.³⁹

II. THE DIPOLE INTERACTION MODEL

Considering a set of N interacting atomic polarizabilities, the atomic induced dipole moment, μ_p^{ind} , due to an external electric field, E^{ext} , is given by

$$\mu_{p,\alpha}^{\text{ind}} = \alpha_{p,\alpha\beta} \left(E_\beta^{\text{ext}} + \sum_{q \neq p}^N T_{pq,\beta\gamma}^{(2)} \mu_{q,\gamma}^{\text{ind}} \right), \quad (1)$$

where $T_{pq,\beta\gamma}^{(2)}$ is the so-called dipole interaction tensor given as

$$T_{pq,\beta\gamma}^{(2)} = \frac{3r_{pq,\beta} r_{pq,\gamma}}{r_{pq}^5} \frac{\delta_{\beta\gamma}}{r_{pq}^3}. \quad (2)$$

In Eq. (1) the Einstein summation convention for repeated indices has been employed, and it is used throughout this work. The molecular polarizability can be written as²²

$$\alpha_{\alpha\beta}^{\text{mol}} = \sum_{p,q}^N B_{pq,\alpha\beta}, \quad (3)$$

where \mathbf{B} is the relay matrix defined in a supermatrix notation as

$$\mathbf{B} = (\boldsymbol{\alpha}^{-1} - \mathbf{T}^{(2)})^{-1}. \quad (4)$$

If we consider two interacting atoms, p and q , the polarizability parallel, α_{\parallel} , and perpendicular, α_{\perp} , to the axes connecting the atoms are given by Silberstein's equations²⁶

$$\alpha_{\parallel} = \frac{\alpha_p + \alpha_q + 4\alpha_p\alpha_q/r^3}{1 - 4\alpha_p\alpha_q/r^6}, \quad (5)$$

$$\alpha_{\perp} = \frac{\alpha_p + \alpha_q - 2\alpha_p\alpha_q/r^3}{1 - \alpha_p\alpha_q/r^6}. \quad (6)$$

Inspection of Eqs. (5) and (6) shows that when r approaches $(4\alpha_p\alpha_q)^{1/6}$, α_{\parallel} goes to infinity and it becomes negative for even shorter distances. Thole avoided this "polarizability catastrophe" by modifying the dipole interaction tensor using smeared-out dipoles.²⁸ The interaction tensor was first written in terms of a reduced distance $u_{pq,\beta} = r_{pq,\beta}/(\alpha_p\alpha_q)^{1/6}$ as

$$T_{pq,\beta\gamma}^{(2)} = (\alpha_p\alpha_q)^{1/2} t(u_{pq}) = (\alpha_p\alpha_q)^{1/2} \frac{\partial^2 \phi(u_{pq})}{\partial u_{pq,\beta} \partial u_{pq,\gamma}}, \quad (7)$$

where $\phi(u_{pq})$ is a spherically symmetric potential of some model charge distribution ρ . Thole considered several different forms of the charge distribution and obtained the most promising results using an interaction tensor of the form,

$$T_{pq,\beta\gamma}^{(2)} = \frac{3v_{pq}^4 r_{pq,\beta} r_{pq,\gamma}}{r_{pq}^5} - \frac{(4v_{pq}^3 - 3v_{pq}^4) \delta_{\beta\gamma}}{r_{pq}^3}, \quad (8)$$

where $v_{pq} = r_{pq}/s_{pq}$ if $r_{pq} < s_{pq}$, otherwise $v_{pq} = 1$ and the normal dipole interaction tensor is recovered. Thole originally defined $s_{pq} = a(\alpha_p \alpha_q)^{1/6}$ with a global damping parameter a . We recently investigated a slightly modified definition, namely $s_{pq} = (\Phi_p \Phi_q)^{1/4}$ where Φ_p is a fitting parameter assumed to be proportional to the atomic second-order moment,³⁴ thereby introducing in an *ad hoc* fashion atom-type damping parameters. Here, this model will be termed the IM-MT model, where IM denotes interaction model and MT denotes modified Thole.

The modification of the interaction tensor in Eq. (8) leads to a tensor with a trace different from zero. The undamped interaction tensor is traceless and the importance of this can be illustrated by considering the molecular quadrupole moment. The quadrupole moment is often chosen as being traceless,⁴⁰ and one reason for this is that its trace does not contribute to the interaction energy according to classical electrostatics. This is noticed from regarding the interaction between a test charge and a quadrupole moment, $1/3q_A T_{AB,\alpha\beta}^{(2)} Q_{B,\alpha\beta}$ and adding a small contribution Δ to each of the diagonal components of $Q_{B,\alpha\beta}$. The additional contribution from Δ to the interaction energy is obtained as

$$\frac{1}{3}q_A \Delta (T_{AB,xx}^{(2)} + T_{AB,yy}^{(2)} + T_{AB,zz}^{(2)}), \quad (9)$$

which normally is zero because $T_{AB,\alpha\beta}^{(2)}$ is traceless. The non-traceless tensor will in principle not give wrong polarizabilities, but the choice will affect the obtained values of the fitted parameters. However, in order to retain the property of $T^{(2)}$ as being traceless, we introduce the damping in a different way. In particular, this will be of importance if the interaction model is extended to molecular dipole–quadrupole polarizabilities and dipole–dipole hyperpolarizabilities. For example, the leading term to an interaction model for the first hyperpolarizability, β , arises from an atomic dipole–quadrupole hyperpolarizability,⁴¹ and includes normally a traceless definition of the quadrupole moment. However, the traceless definition of the quadrupole moment has been criticized because some electromagnetic observables apparently become origin-dependent for this choice of definition.⁴²

Damping may be included by modifying the distance r_{pq} to obtain a scaled distance, s_{pq} ,

$$s_{pq} = v_{pq} r_{pq} = f(r_{pq}), \quad (10)$$

where v_{pq} is a scaling factor and $f(r_{pq})$ is an appropriately chosen function of r_{pq} . Furthermore, if each component of r_{pq} also is scaled by v_{pq} , the reduced distance becomes

$$s_{pq} = \sqrt{s_{pq,\alpha} s_{pq,\alpha}} = v_{pq} \sqrt{r_{pq,\alpha} r_{pq,\alpha}} = v_{pq} r_{pq}, \quad (11)$$

which is consistent with the definition in Eq. (10). The interaction tensor can thus be obtained from

$$T_{pq,\alpha_1 \dots \alpha_n}^{(n)} = \nabla_{\alpha_1} \dots \nabla_{\alpha_n} \left(\frac{1}{s_{pq}} \right), \quad (12)$$

which is equivalent to replacing r_{pq} by s_{pq} and $r_{pq,\alpha}$ by $s_{pq,\alpha}$ in the regular formulas for the interaction tensor.

To derive explicit formulas for the scaling function $f(r_{pq})$ we consider the interaction between two spherical Gaussian charge distributions with exponents Φ_p and Φ_q and normalized to one. The interaction energy is given by^{43,44}

$$V = \int \int \frac{\rho_p(r_1) \rho_q(r_2)}{r_{12}} dr_1 dr_2 = \frac{\text{erf}(\sqrt{a} r_{pq})}{r_{pq}}, \quad (13)$$

where a is the reduced exponent $a = \Phi_p \Phi_q / (\Phi_p + \Phi_q)$ and $\text{erf}(\sqrt{a} r_{pq})$ is the regular error function. As the exponent $\sqrt{a} r_{pq}$ tends to infinity, the error function tends to 1 and we recover the usual expression for a point charge. This leads to a scaling function of the form

$$f(r_{pq}) = \frac{r_{pq}}{\text{erf}(\sqrt{a} r_{pq})}. \quad (14)$$

The components of the scaled distance vector, $s_{pq,\alpha}$, are calculated as $v_{pq} r_{pq,\alpha}$, where v_{pq} is obtained from Eq. (10) as

$$v_{pq} = \frac{f(r_{pq})}{r_{pq}}. \quad (15)$$

However, due to the relatively complex form of the error function we have also investigated two approximations of this function,⁴⁵ namely

$$f(r_{pq}) = \sqrt{r_{pq}^2 + \frac{\pi}{4a}} \quad (16)$$

and

$$f(r_{pq}) = \left(r_{pq}^4 + \frac{\pi^2}{16a^2} \right)^{-1/4}. \quad (17)$$

The approximations in Eqs. (16) and (17) can be realized considering the limits of Eq. (13) at $r_{pq} \rightarrow 0$ and $r_{pq} \rightarrow \infty$, i.e.,

$$\lim_{r_{pq} \rightarrow \infty} \frac{\text{erf}(\sqrt{a} r_{pq})}{r_{pq}} = \frac{1}{r_{pq}} \quad (18)$$

and

$$\lim_{r_{pq} \rightarrow 0} \frac{\text{erf}(\sqrt{a} r_{pq})}{r_{pq}} = \frac{1}{\sqrt{\frac{\pi}{4a}}}. \quad (19)$$

To give the correct limiting behavior, the combination of Eqs. (18) and (19) may lead to either Eqs. (16) or (17). The three different models will be denoted according to the scaling function used i.e., IM-ERF, IM-SQRT, or IM-QDRT if, respectively, Eqs. (14), (16), or (17) is used. It is noted that in particular the form of the damping in Eq. (16) would be efficient in molecular dynamics simulations of condensed phases because in principle it only involves an extra addition in the calculation of the distance.

Well below the first electronic absorption, the frequency dependence of the molecular polarizability is often approxi-

mated with an Unsöld-type of expression.⁶ Here we assume that the atomic polarizability has a similar frequency dependence,³⁴

$$\alpha_p(-\omega; \omega) = \alpha_p(0; 0) \times \left[\frac{\bar{\omega}_p^2}{\bar{\omega}_p^2 - \omega^2} \right], \quad (20)$$

where $\bar{\omega}_p$ is an atom-type parameter and ω is the frequency.

III. QUANTUM CHEMICAL CALCULATION

The quantum chemical computations of frequency-dependent polarizabilities were carried out with the DALTON program package⁴⁶ as described in Refs. 10, 47, 48 using linear response functions at the self-consistent field (SCF) level. The basis set of Sadlej⁴⁹ was employed because it has been shown previously that it gives good results for polarizabilities considering its limited size.²¹ The following frequencies have been used: $\omega(\text{a.u.})/\lambda(\text{nm}) = 0.0/\infty$, 0.023 89/1907, 0.042 82/1064, and 0.0774/589 (1 a.u. = 27.21 eV). A series of 74 molecules has been generated from four disubstituted six-membered heteromonocyclic compounds containing B, N, and C atoms.⁵⁰ The heterorings investigated were borazine, 1,3,5-triborate, hexahydro-1,3,5-triazine, and hexahydro-1,4-diboro-2,5-diazine where the nomenclature used is the extended Hantzsch–Widman system.⁵¹ The geometry of the substituted heterorings were optimization at the PM3 level with the GAUSSIAN 94 program package.⁵² The set of 74 heterorings were added to the set of 113 molecules (the original set of 115 molecules apart from the two biphenyls) used in the previous study of aliphatic and aromatic molecules.³⁴ The geometry of the molecules in the original

set was generated adopting standard bond lengths and bond angles taken from Refs. 53 and 54. We have not included olephines in the trial set since in this case intramolecular charge-transfer effects are important, and these effects cannot be modeled on the basis of atomic polarizabilities only.^{55–57} It is noted that we use different kinds of molecular geometries for different molecules. The obtained atomic parameters should, however, be independent of the choice of molecular geometry because the geometry dependence is included explicitly in the $T^{(2)}$ tensor [see Eq. (2)]. In contrast, for applications the choice of molecular geometries can be crucial in the comparison of model results with experimental data. A crucial test of the atomic parameters would be to calculate polarizability derivatives and thereby Raman scattering parameters in line with the work by Applequist and Quicksall.^{23,58}

The parameters describing the frequency-dependent polarizabilities have been optimized using the same scheme as in Ref. 34. For the static polarizability, the rms of the differences between the quantum chemical molecular polarizability tensors, $\alpha_{\alpha\beta,i}^{\text{QC}}$, and the model molecular polarizability tensors, $\alpha_{\alpha\beta,i}^{\text{model}}$, is minimized as

$$\text{rms} = \sqrt{\frac{\sum_{i=1}^N \sum_{\alpha,\beta=1}^3 (\alpha_{\alpha\beta,i}^{\text{model}} - \alpha_{\alpha\beta,i}^{\text{QC}})^2}{N-1}}, \quad (21)$$

where N is the number of molecules.

The parameters describing the frequency dependence of the molecular polarizability have been optimized by minimizing

$$\text{rms} = \sqrt{\frac{\sum_{i=1}^N \sum_{\alpha,\beta=1}^3 [(\alpha_{\alpha\beta,i}^{\text{model}}(\omega) - \alpha_{\alpha\beta,i}^{\text{model}}(0)) - (\alpha_{\alpha\beta,i}^{\text{QC}}(\omega) - \alpha_{\alpha\beta,i}^{\text{QC}}(0))]^2}{N-1}}, \quad (22)$$

i.e., we parametrize the frequency dependence only and do not attempt to correct for errors introduced in the parametrization of the static polarizability.

The *interaction* polarizability, $\Delta\alpha$, was calculated as the difference between the dimer polarizability and twice the monomer polarizability as

$$\Delta\alpha = \alpha^{\text{dimer}} - 2\alpha^{\text{monomer}}, \quad (23)$$

and for the SCF calculations on the complexes, we corrected for basis set superposition errors by the counterpoise method.⁵⁹ Four different kinds of dimers were included in the study. The HF dimer has a single hydrogen bond whereas the linear urea dimer forms two hydrogen bonds. In addition, two nonpolar complexes, the methane and benzene dimers, are included where the attractive part of the interaction is dominated by dispersion interactions. In the case of the benzene dimer, it was arranged such that the π electrons are perturbed, which is not the most likely orientation but it serves as a severe test of the model. The relative orientations of the molecules in the dimers are displayed in Fig. 1. It

should be noted that the interaction polarizabilities are often rather small compared with the molecular polarizability and they will therefore be critical tests of the model. The HF, methane, and benzene molecules have been included in the

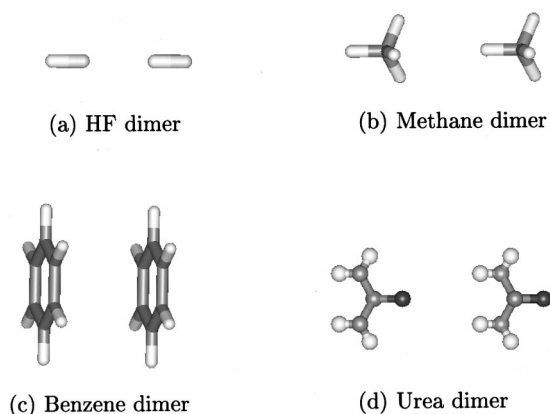


FIG. 1. Relative orientation of the four dimers.

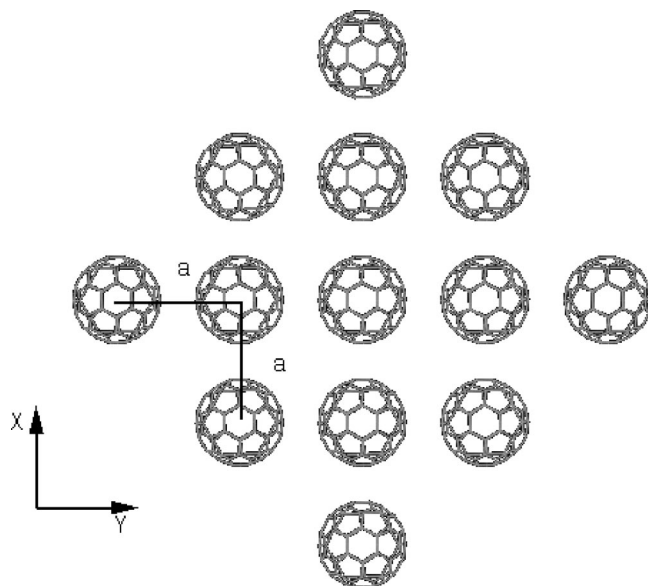


FIG. 2. The two-dimensional C_{60} cluster with 13 molecules. The distance between nearest molecules is $a = 10.02 \text{ \AA}$.

training-set described previously, whereas the urea molecule was not included. The geometry of the urea molecules was taken from Ref. 60. For the calculations on the urea chains, the intermolecular distance between the centers of mass of the urea molecules in the planar urea chains is 9.5 bohr, which corresponds to the equilibrium distance of the linear dimer.⁶¹ The structure of the C_{60} molecule was taken from our previous work.³⁵ Solid C_{60} exhibits a face-centered-cubic structure with a lattice vector $a_0 = 14.17 \text{ \AA}$ giving a nearest-neighbor distance of $a = 10.02 \text{ \AA}$.⁶² The one- and two-dimensional clusters were constructed using this nearest-neighbor distance and the two-dimensional structure is illustrated in Fig. 2.

IV. RESULTS

The optimized parameters describing the static polarizability for the IM-MT, IM-ERF, IM-QDRT, and IM-SQRT models are given in Table I, where also the parameters from our previous work³⁴ on the IM-MT model are included. A

detailed comparison with the Applequist model and the Thole model has not been carried out here but can be found in, e.g., Ref. 34.

For the IM-MT model, which includes the additional heterocyclic molecules in comparison with our previous work, we find that the inclusion of the heterocyclic molecules in the training set does not reduce the accuracy of the model. However, the actual values of the parameters change considerably, and in particular the damping parameters are different. For the polarizability parameters, the largest changes are found for α_N . The reason is that all added molecules contain BN-ring systems, which means that we have added a new type of nitrogen-containing molecule. This indicates that damping is especially important for ring systems, which is also discussed by Applequist⁵⁶ in his *partial neglect of ring interactions* (PNRI) approximation for aromatic molecules. In the PNRI approximation, C is assigned an anisotropic polarizability (components parallel and perpendicular to the ring) and interactions between carbon atoms in the same conjugated system are neglected. The PNRI approximation is required in the Applequist model in order to get a reasonable description of the polarizability perpendicular to the ring in aromatic molecules.

As noticed in Table I, the values of the polarizability parameters are lowered for the approaches included here (IM-ERF, IM-QDRT, IM-SQRT), but this is compensated by modifying the damping parameters. In general, it seems like the damping parameters are more affected by the choice of training set, optimizing procedure, etc., than the atomic polarizabilities. Both the polarizability and damping parameters are very similar for all three models as expected due to the similarity of the damping functions. The best fit is obtained for the simplest model, IM-SQRT, although no significant difference between the IM-SQRT model and the IM-QDRT model is found. Compared with the IM-MT model, the IM-SQRT model gives an improvement of around 15%, which is substantial considering that only the damping function has been changed and no additional fitting parameters have been included.

The relative mean absolute error (mae) in the diagonal components is also presented in Table I. It should be noted that the rms includes both diagonal and off-diagonal compo-

TABLE I. Atomic parameters fitted to model the static polarizability (in a.u., 1 a.u. = 0.1482 \AA^3).

Atom	IM-MT				IM-ERF		IM-QDRT		IM-SQRT	
	α_p	Φ_p	α_p^a	Φ_p^a	α_p	Φ_p	α_p	Φ_p	α_p	Φ_p
H	2.118	1.090	1.84	2.75	1.335	0.267	1.310	0.336	1.280	0.358
B	10.612	9.475	8.782	0.047	8.611	0.075	8.649	0.074
C	11.111	7.600	11.52	20.99	8.405	0.083	8.415	0.124	8.465	0.124
N	8.365	6.491	10.55	26.55	5.994	0.177	6.127	0.274	6.169	0.268
O	6.982	3.825	5.64	12.16	3.626	2.794	3.805	2.649	3.754	4.103
F	2.603	1.752	2.25	4.78	1.967	1.667	1.937	1.653	1.907	1.468
Cl	15.342	4.921	16.08	17.64	13.101	0.185	13.084	0.468	13.081	0.453
rms ^b	6.29		6.67		5.71		5.30		5.29	
mae ^c	4.98 ± 2.98%		...		3.71 ± 2.66%		3.50 ± 2.56%		3.55 ± 2.60%	

^aSee Ref. 34. Fitted to 115 aliphatic and aromatic molecules.

^bOptimized error, see Eq. (21).

^cMean absolute error in diagonal components.

TABLE II. Parameters describing the frequency dependence of molecular polarizabilities (in a.u.).

Atom	All molecules		Aliphatic		Aromatic		Boron
	$\bar{\omega}_p$	$\bar{\omega}_p^a$	$\bar{\omega}_p$	$\bar{\omega}_p^a$	$\bar{\omega}_p$	$\bar{\omega}_p^a$	$\bar{\omega}_p$
H	0.471	0.605	0.413	0.414	0.341	0.351	1.081
B	0.446	0.467
C	0.541	0.445	0.784	0.714	0.447	0.396	0.596
N	0.811	0.342	0.658	0.432	0.295	0.223	0.649
O	0.386	0.561	0.493	0.430	1.773	1.339	0.408
F	0.311	0.404	0.896	0.973	1.934	1.085	1.149
Cl	0.461	0.441	0.532	0.530	0.544	0.432	0.535
rms	1.286	0.809	0.375	0.424	0.559	0.712	0.582

^aTaken from Ref. 34.

nents. The IM-QDRT model gives the lowest mae but again there is little difference between the IM-SQRT and IM-QDRT models. The IM-SQRT is therefore expected to give results which are within 6% of the SCF results.

If the atomic parameters are compared, it is found for the IM-MT model that α_B is slightly smaller than α_C , which is unphysical. In contrast, for the three new models α_B is slightly larger than α_C . The differences are, however, small and changes in the α parameters may be compensated by modifying the Φ parameters. For the three new models, it is also noted that in particular Φ_O but also Φ_F are considerably larger than the other Φ parameters. This can be understood since the damping term $1/a$ can be rewritten as $1/a = 1/\Phi_p + 1/\Phi_q$ and therefore the smallest damping parameter will to a large extent determine the damping. Even if one may regard the Φ parameters as a measure of an atomic second moment, it is, as already mentioned, our experience that the actual values of the Φ parameters are sensitive to the optimization procedure. Presently, it is therefore difficult to regard the Φ parameters as anything else than fitting parameters.

In Table II, we present the parameters describing the frequency dependence of the polarizability. As in our previous work,³⁴ we find a significant improvement by dividing the molecules in the training set into three groups, i.e., aliphatic, aromatic, and molecules containing the element B. It is interesting that improvements were found by separating the BN rings into its own group. It may be related to the special electro-optic properties found for boron–nitride tubes (see, e.g., Ref. 39 and references therein). The rms values are reduced by almost a factor of 2 for all three groups as compared to including all molecules in one group. In general, we find good agreement with the results from our previous work.³⁴ For the aliphatic molecules the largest changes are found for the $\bar{\omega}^N$ parameter. This is due to the fact that the hexahydro-1,3,5-triazine rings have been added to this group. The fact that the rest of the parameters are only slightly affected illustrates the transferability of the parameters. In the case of the group of aromatic molecules, large changes are found for $\bar{\omega}^O$ and $\bar{\omega}^F$ parameters. Since the set of aromatic molecules employed in this work are the same as in the previous study, the changes are due to minor differences in the optimization routine used. The reason for this is that $\bar{\omega}^O$ and $\bar{\omega}^F$ have the largest values. Therefore, they give an almost negligible contribution to the total frequency depen-

dence of the polarizability [see Eq. (20)] and are not very well determined in the optimization. It is demonstrated that the frequency dependence of the molecular polarizability for the heterorings can also be described with atom-type parameters. However, for the boron group in particular the H parameter is different from the other groups. Equivalently to the previous discussion, $\bar{\omega}_H$ has become so large that it is not contributing to the frequency dependence. Qualitatively, it should not be expected that the electrons related to the hydrogen atoms contribute to the frequency dependence for these molecules because the most important absorption band is related to the ring structure.

A. Dimers

The interaction polarizabilities of the HF, methane, benzene, and urea dimers are displayed in Figs. 3, 4, 5, and 6, respectively. The interaction polarizability calculated with the IM-SQRT model is compared with SCF results. For the HF dimer (Fig. 3), the results of the IM-MT model are also included in order to illustrate the discontinuous damping function of the IM-MT model. From the discontinuity in Fig. 3, we see that in the IM-MT model there is no damping for distances larger than 2 bohr. This is expected since the

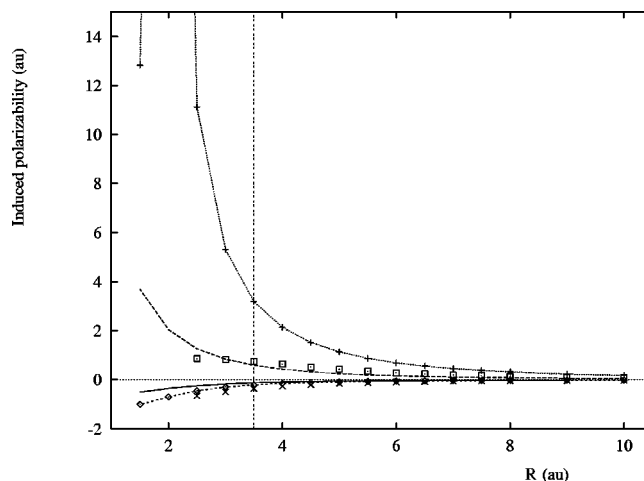


FIG. 3. Interaction polarizability of the HF dimer in a.u. SCF results: (\square) α_{\parallel} and (\times) α_{\perp} . IM-MT results: (\cdots , $+$) α_{\parallel} and (\cdots , \diamond) α_{\perp} . IM-SQRT results: ($---$) α_{\parallel} and ($---$) α_{\perp} . Vertical line indicates equilibrium distance taken from Ref. 80.

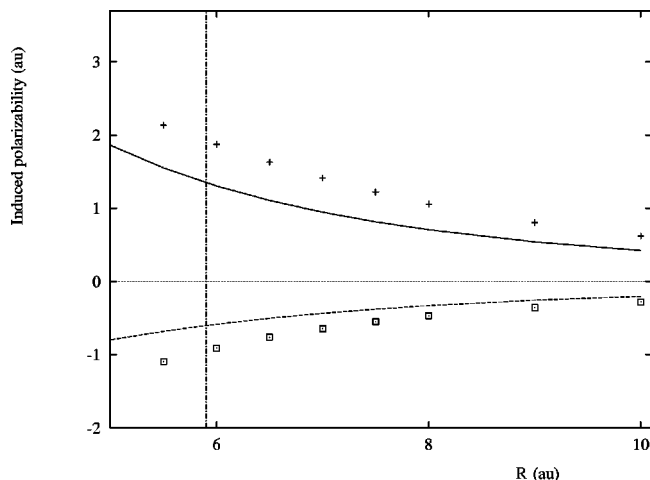


FIG. 4. Interaction polarizability of the methane dimer in a.u. SCF results: (+) α_{\parallel} and (\square) α_{\perp} . IM-SQRT results: (—) α_{\parallel} and (---) α_{\perp} . Vertical line indicates equilibrium distance taken from Ref. 81.

IM-MT model is optimized to reproduce damping effects at typical bond distances for covalent bonds and not at typical intermolecular distances. Using the IM-SQRT model improves the damping greatly at short intermolecular distances for the HF dimer. Although the discontinuity in the IM-MT models only occurs at very short intermolecular distances, it may still not be suitable for being used in molecular dynamics simulations as discussed by Burnham *et al.*³³ For the other three dimers (Figs. 4–6) the IM-SQRT model slightly overestimates the intermolecular damping which again is due to the fact that the IM-SQRT model is optimized to describe damping at intramolecular bond distances. Furthermore, it is observed that the SCF results predict that the interaction polarizability of the benzene and HF dimer parallel to the separation axes become almost stationary around the equilibrium distance. This behavior cannot be reproduced with the damping function employed here.

In spite of the chemical difference of the four dimers studied some general trends are found for the interaction po-

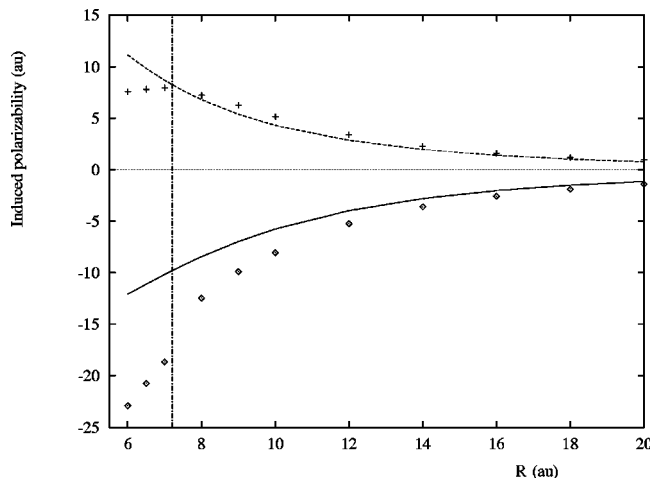


FIG. 5. Interaction polarizability of the benzene dimer in a.u. SCF results: (+) α_{\parallel} and (\diamond) α_{\perp} . IM-SQRT results: (---) α_{\parallel} and (—) α_{\perp} . Vertical line indicates equilibrium distance taken from Ref. 82.

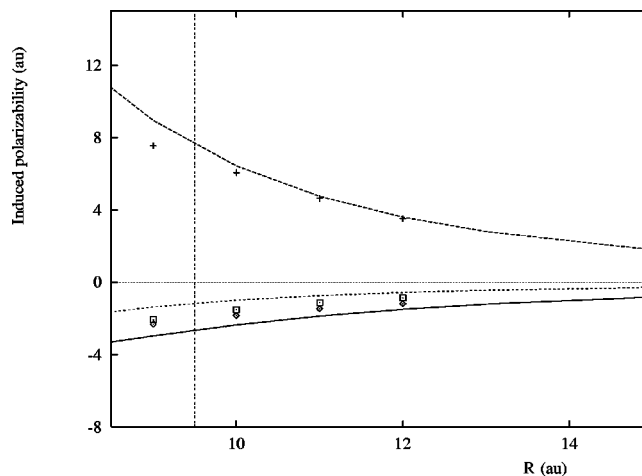


FIG. 6. Interaction polarizability of the urea dimer in a.u. SCF results: (+) α_{\parallel} , (\diamond) α_{\perp} in plane and (\square) α_{\perp} out of plane. IM-SQRT results: (---) α_{\parallel} , (—) α_{\perp} in plane and (---) α_{\perp} out of plane. Vertical line indicates equilibrium distance taken from Ref. 61.

larizability. The interaction polarizability of the dimers increases in the direction along the axes connecting the molecules (“dimer axes”) and decreases in the directions perpendicular to the dimer axes, which is expected from Eqs. (5) and (6). The mean polarizability is, however, almost unchanged by the intermolecular interactions. That the isotropic part of the polarizability is almost additive for a linear dimer may be realized from Eqs. (5) and (6). If a diatomic molecule, consisting of atoms p and q , is considered, the isotropic part of the polarizability is $\alpha = \frac{1}{3}(\alpha_{\parallel} + 2\alpha_{\perp})$, which becomes $\alpha = \alpha_p + \alpha_q$ if the short-range $1/r^6$ terms in the denominator of Eqs. (5) and (6) are neglected. The agreement between the IM-SQRT model and the SCF results is in general reasonable over a wide range of intermolecular distances. The largest discrepancy is found at short distances for the benzene dimer perpendicular to the separation axes (see Fig. 5). This was expected due to the nonclassical effects arising from perturbations of the π system in the benzene dimer at short distances. At large intermolecular distances,

TABLE III. Polarizability of urea chains calculated using IM-SQRT (in a.u.). N is the number of molecules in the chain. Y axes are along the chain, X axes are perpendicular to the chain but in the plane and Z axes are perpendicular to the plane.

N	α_{xx}^a	α_{zz}^a	α_{yy}^a	$\bar{\alpha}^a$
1	39.68	22.09	38.23	33.33
2	76.69 (−3.4)	43.01 (−2.6)	84.03 (9.9)	67.91 (1.9)
4	149.97 (−5.5)	84.59 (−4.3)	179.51 (17.4)	138.02 (3.5)
6	223.03 (−6.3)	126.11 (−4.9)	276.10 (20.4)	208.41 (4.2)
8	296.03 (−6.7)	167.60 (−5.2)	372.97 (21.9)	278.87 (4.6)
10	369.01 (−7.0)	209.09 (−5.3)	469.94 (22.9)	349.35 (4.8)
15	551.42 (−7.4)	312.79 (−5.6)	712.55 (24.3)	525.59 (5.1)
20	733.81 (−7.5)	416.49 (−5.7)	955.27 (24.9)	701.86 (5.3)
30	1 098.55 (−7.7)	623.87 (−5.9)	1 440.79 (25.6)	1 054.40 (5.5)
50	1 828.01 (−7.9)	1 038.63 (−6.0)	2 411.94 (26.2)	1 759.53 (5.6)
100	3 651.61 (−8.0)	2 075.51 (−6.0)	4 839.99 (26.6)	3 522.37 (5.7)
200	7 298.78 (−8.0)	4 149.26 (−6.1)	9 696.18 (26.8)	7 048.07 (5.7)
300	10 945.95 (−8.0)	6 223.00 (−6.1)	14 552.39 (26.9)	10 573.78 (5.7)

^aPercent deviation from additivity in parentheses.

TABLE IV. Polarizability of C_{60} calculated using IM-SQRT (in a.u.). N is the number of molecules in the cluster.

N	One-dimensional cluster			Two-dimensional cluster		
	α_{\perp}^a	α_{\parallel}^a	$\bar{\alpha}/N^a$	α_{\perp}^a	α_{\parallel}^a	$\bar{\alpha}/N^a$
1	522.62	522.62	522.62
2	981.71 (-6.1)	1 231.67 (17.8)	532.52 (1.9)
3	1 434.69 (-8.5)	1 994.32 (27.2)	540.41 (3.4)
5	2 336.31 (-10.6)	3 568.27 (36.6)	549.39 (5.1)	2273.72 (-13.0)	2 919.66 (11.7)	540.87 (3.5)
7	3 236.09 (-11.5)	5 162.48 (41.1)	554.03 (6.0)
13	5 932.65 (-12.7)	9 971.86 (46.8)	559.93 (7.1)	5410.12 (-20.4)	8 118.21 (19.5)	555.04 (6.2)
25	11 323.15 (-13.3)	19 612.55 (50.1)	563.45 (7.8)	9879.24 (-24.4)	16 284.52 (24.6)	565.98 (8.3)

^aPercent deviation from additivity in parentheses.

the difference between the SCF results and the IM-SQRT model becomes small. This indicates that the long-range induced polarizability at the SCF level is well described in terms of dipole-induced-dipole interactions in good agreement with the result on the He dimer.⁶³ The results for the interaction polarizability of the HF dimer compare well with that obtained from the equilibrium structure of the HF dimer which is bent compared with the linear dimer structure adopted here.⁶⁴ Similar trends for the interaction polarizability are also observed for the linear acetylene dimer,⁶⁵ the linear dimer of H_2NO ,⁶⁶ the water dimer,⁶⁷ the linear dimer of urea,⁶⁸ and parallel chains of polyacetylene oligomers.⁶⁹ Also, since a similar behavior is observed for the second hyperpolarizability^{65,69,70} this indicates a general scheme for enhancing the (hyper)polarizability of assemblies of molecules by aligning the molecules along the axes with the largest polarizability. Furthermore, interactions between different chains should be minimized since these interactions tend to lower the polarizability.⁶⁹ However, further studies of the interaction (hyper)polarizability are needed in order to determine the usefulness of this type of alignment scheme.

B. Chain of urea molecules

The polarizability of chains of urea molecules with increasing number of molecules in the chain and their deviation from additivity are presented in Table III. The mean polarizability, $\bar{\alpha}$, is defined as $\bar{\alpha} = \frac{1}{3}(\alpha_{xx} + \alpha_{yy} + \alpha_{zz})$. With increasing number of molecules, we find that the polarizability parallel to the chain increases more than expected from an additive model and perpendicular to the chain it increases less rapidly than an additive model. A significant deviation from additivity is found for the tensor component along the chain which amounts to around 25%. For the mean polarizability, however, the largest deviation from additivity is around 5%. These results are in good agreement with the *ab initio* study of Perez and Dupuis⁶⁸ on urea dimers and trimers. A chain length of around 100 molecules is needed before the deviation from additivity becomes stationary. Since the polarizability is converging slowly with respect to the number of molecules in the chain, extrapolation schemes are often employed to get the polarizability in the infinite limit. However, the polarizability for infinitely long chains is dependent on both the adopted extrapolation scheme and the total number of entities.⁷¹

C. C_{60} clusters

For C_{60} , we have investigated the polarizability both for one- and two-dimensional clusters. The results are presented in Table IV and again the deviation from additivity is given in parentheses. The polarizability components parallel to the chain and in the plane of the film increase more rapidly with the number of molecules than expected from an additive model, whereas the components perpendicular to the chain and out of the plane increase less rapidly than an additive model. The deviation from additivity is larger for the chain than for the film. It is around 50% along the chain and around -15% perpendicular to the chain. In the case of the two-dimensional cluster the relative deviations from additivity perpendicular to the plane and in the plane are nearly identical but with different sign. The largest deviation from additivity in the mean polarizability is around 8% both for the chain and the film.

The mean polarizability of the isolated C_{60} molecule is calculated to 77.5 \AA^3 , which agrees well with the experimental result of $76.5 \pm 8 \text{ \AA}^3$ (Ref. 72) and an accurate SCF result of 75.1 \AA^3 .⁷³ In addition, good agreement is found between the results of the largest two-dimensional cluster of 83.9 \AA^3 and experimental results on thin films where the results range between 80.5 and 91.9 \AA^3 .⁷⁴⁻⁷⁹ The experimental estimate of the vibrational contribution to the polarizability is only about 2 \AA^3 ,⁷⁹ indicating that our model gives reasonable results for C_{60} clusters as compared to experiments.

V. CONCLUSIONS

In this work, we have investigated an approach for modeling the damping contribution in the dipole interaction model. In contrast to the Thole model, the interaction tensors in this approach remain traceless. The modification discussed here also gives a significant improvement compared with the models adopted in previous work, even though also heterocyclic compounds have been included in the model. Although the model can describe the frequency-dependent molecular polarizability with one parameter for each element describing the frequency dependence, a significant improvement is found by dividing the molecules into aliphatic, aromatic, and molecules containing the element B.

The interaction polarizability of four dimers has also been studied. We find in general good agreement between the model and the SCF results over a wide range of intermolecu-

lar distances. Polarizabilities of linear chains of urea molecules and one- and two-dimensional clusters of C_{60} molecules have also been calculated. The effects of neighboring molecules on the polarizability anisotropy are substantial, whereas the effects are smaller on the mean polarizability. For the mean polarizability of C_{60} , we find good agreement between the model and experiments both in the case of an isolated molecule and a model of a thin film. The Cartesian coordinates and quantum chemical molecular polarizability tensors for the molecules in the training set can be found in Ref. 83.

ACKNOWLEDGMENTS

L.J. thanks Professor Paolo Lazzeretti for kindly supplying the Sadlej basis set for boron. L.J. gratefully acknowledges The Danish Research Training Council for financial support. K.V.M. thanks Statens Naturvidenskabelige Forskningsråd (SNF), Statens Teknisk-Videnskabelige Forskningsråd (STVF) and the EU-network:MOLPROP for support.

¹P. N. Prasad and D. J. Williams, *Introduction to Nonlinear Optical Effects in Molecules and Polymers* (Wiley, New York, 1991).

²P. Ball, *Made to Measure, New Materials for the 21st Century* (Princeton University Press, Princeton, NJ, 1997).

³*Molecular Electronics*, edited by J. Jortner and M. Ratner (Blackwell Science, Oxford, 1997).

⁴D. P. Shelton and J. E. Rice, *Chem. Rev.* **94**, 3 (1994).

⁵D. R. Kanis, M. A. Ratner, and T. J. Marks, *Chem. Rev.* **94**, 195 (1994).

⁶D. M. Bishop, *Adv. Quantum Chem.* **25**, 1 (1994).

⁷Y. Luo, H. Agren, P. Jørgensen, and K. V. Mikkelsen, *Adv. Quantum Chem.* **26**, 165 (1995).

⁸I. D. L. Albert, T. J. Marks, and M. A. Ratner, *J. Phys. Chem.* **100**, 9714 (1996).

⁹S. P. Karna, *J. Phys. Chem. A* **104**, 4671 (2000).

¹⁰J. Olsen and P. Jørgensen, *J. Chem. Phys.* **82**, 3235 (1985).

¹¹B. Champagne, E. A. Perpète, S. J. A. van Gisbergen, E.-J. Baerends, J. G. Snijders, C. Soubra-Ghaoui, K. A. Robins, and B. Kirtman, *J. Chem. Phys.* **109**, 10489 (1998).

¹²S. J. A. van Gisbergen, P. R. T. Schipper, O. V. Gritsenko, E. J. Baerends, J. G. Snijders, B. Champagne, and B. Kirtman, *Phys. Rev. Lett.* **83**, 694 (1999).

¹³L. Silberstein, *Philos. Mag.* **33**, 92 (1917).

¹⁴K. G. Denbigh, *Trans. Faraday Soc.* **36**, 936 (1940).

¹⁵B. C. Vickery and K. G. Denbigh, *Trans. Faraday Soc.* **45**, 61 (1949).

¹⁶K. J. Miller and J. A. Savchik, *J. Am. Chem. Soc.* **101**, 7206 (1979).

¹⁷Y. K. Kang and M. S. Jhon, *Theor. Chim. Acta* **61**, 41 (1982).

¹⁸K. J. Miller, *J. Am. Chem. Soc.* **112**, 8533 (1990).

¹⁹J. M. Stout and C. E. Dykstra, *J. Am. Chem. Soc.* **117**, 5127 (1995).

²⁰J. M. Stout and C. E. Dykstra, *J. Phys. Chem. A* **102**, 1576 (1998).

²¹K. O. Sylvester-Hvid, P.-O. Åstrand, M. A. Ratner, and K. V. Mikkelsen, *J. Phys. Chem. A* **103**, 1818 (1999).

²²J. Applequist, J. R. Carl, and K. F. Fung, *J. Am. Chem. Soc.* **94**, 2952 (1972).

²³J. Applequist, *Acc. Chem. Res.* **10**, 79 (1977).

²⁴K. A. Bode and J. Applequist, *J. Phys. Chem.* **100**, 17820 (1996).

²⁵L. Silberstein, *Philos. Mag.* **33**, 215 (1917).

²⁶L. Silberstein, *Philos. Mag.* **33**, 521 (1917).

²⁷R. R. Birge, *J. Chem. Phys.* **72**, 5312 (1980).

²⁸B. T. Thole, *Chem. Phys.* **59**, 341 (1981).

²⁹R. R. Birge, G. A. Schick, and D. F. Bocian, *J. Chem. Phys.* **79**, 2256 (1983).

³⁰A. H. de Vries, P. T. van Duijnen, R. W. J. Zijlstra, and M. Swart, *J. Electron Spectrosc. Relat. Phenom.* **86**, 49 (1997).

³¹P. T. van Duijnen and M. Swart, *J. Phys. Chem.* **102**, 2399 (1998).

³²A. A. Chialvo and P. T. Cummings, *Fluid Phase Equilib.* **150-151**, 73 (1998).

³³C. J. Burnham, J. Li, S. S. Xantheas, and M. Leslie, *J. Chem. Phys.* **110**, 4566 (1999).

³⁴L. Jensen, P.-O. Åstrand, K. O. Sylvester-Hvid, and K. V. Mikkelsen, *J. Phys. Chem. A* **104**, 1563 (2000).

³⁵L. Jensen, O. H. Schmidt, K. V. Mikkelsen, and P.-O. Åstrand, *J. Phys. Chem. B* **104**, 10462 (2000).

³⁶D. M. Bishop, *Rev. Mod. Phys.* **62**, 343 (1990).

³⁷D. M. Bishop, *Adv. Chem. Phys.* **104**, 1 (1998).

³⁸B. Champagne, *Int. J. Quantum Chem.* **65**, 689 (1997).

³⁹J. Kongsted, A. Osted, L. Jensen, P.-O. Åstrand, and K. V. Mikkelsen, *J. Phys. Chem. B* **105**, 10243 (2001).

⁴⁰A. D. Buckingham, *Adv. Chem. Phys.* **12**, 107 (1967).

⁴¹A. D. Buckingham, E. P. Concannon, and I. D. Hands, *J. Phys. Chem.* **98**, 10455 (1994).

⁴²M. J. Gunning and R. E. Raab, *Mol. Phys.* **91**, 589 (1997).

⁴³S. F. Boys, *Proc. R. Soc. London* **200**, 542 (1950).

⁴⁴T. Helgaker, P. Jørgensen, and J. Olsen, *Molecular Electronic-Structure Theory* (Wiley, Chichester, 2000).

⁴⁵G. A. van der Velde, CECAM Workshop Report, 1972, edited by H. J. C. Berendsen.

⁴⁶T. Helgaker, H. J. Aa. Jensen, P. Jørgensen *et al.*, DALTON, an electronic structure program, Release 1.0 <http://www.kjemi.uio.no/software/dalton>, 1997.

⁴⁷H. J. Aa. Jensen, H. Koch, P. Jørgensen, and J. Olsen, *Chem. Phys.* **119**, 297 (1988).

⁴⁸H. J. Aa. Jensen, P. Jørgensen, and J. Olsen, *J. Chem. Phys.* **89**, 3654 (1988).

⁴⁹A. J. Sadlej, *Collect. Czech. Chem. Commun.* **53**, 1995 (1988).

⁵⁰The 74 molecules are: borazine, 1,2-dichloro-borazine, 2,4-dichloro-borazine, 1,2-difluoro-borazine, 1,4-difluoro-borazine, 2,4-difluoro-borazine, 1-amino-4-nitro-borazine, 2-amino-1-nitro-borazine, 2-amino-4-nitro-borazine, 4-amino-1-nitro-borazine, 1,3,5-triborane, 1,3-difluoro-1,3,5-triborane, 1-amino-3-nitro-1,3,5-triborane, 2-amino-4-nitro-1,3,5-triborane, cis-2,4-dichloro-1,3,5-triborane, cis-2,4-difluoro-1,3,5-triborane, trans-2,4-dichloro-1,3,5-triborane, trans-2,4-difluoro-1,3,5-triborane, 1,2-dichloro-1,3,5-triborane, 1,2-difluoro-1,3,5-triborane, 1-amino-2-nitro-1,3,5-triborane, 1,4-dichloro-1,3,5-triborane, 1,4-difluoro-1,3,5-triborane, 1-nitro-2-amino-1,3,5-triborane, 1-nitro-4-amino-1,3,5-triborane, 1-amino-4-nitro-1,3,5-triborane, hexahydro-1,3,5-triazine, 1,3-dichloro-tetrahydro-1,3,5-triazine, 1,3-difluoro-tetrahydro-1,3,5-triazine, 2-amino-4-nitro-tetrahydro-1,3,5-triazine, cis-2,4-dichloro-tetrahydro-1,3,5-triazine, cis-2,4-difluoro-tetrahydro-1,3,5-triazine, trans-2,4-dichloro-tetrahydro-1,3,5-triazine, trans-2,4-difluoro-tetrahydro-1,3,5-triazine, 1,2-dichloro-tetrahydro-1,3,5-triazine, 1-amino-2-nitro-tetrahydro-1,3,5-triazine, 2-amino-1-nitro-tetrahydro-1,3,5-triazine, 1,4-dichloro-tetrahydro-1,3,5-triazine, 1-amino-4-nitro-tetrahydro-1,3,5-triazine, 4-amino-1-nitro-tetrahydro-1,3,5-triazine, hexahydro-1,4-dibora-2,5-diazine, 1,3-dichloro-tetrahydro-1,4-dibora-2,5-diazine, 1,5-dichloro-tetrahydro-1,4-dibora-2,5-diazine, 3,5-dichloro-tetrahydro-1,4-dibora-2,5-diazine, 1,3-difluoro-tetrahydro-1,4-dibora-2,5-diazine, 1,5-difluoro-tetrahydro-1,4-dibora-2,5-diazine, 3,5-difluoro-tetrahydro-1,4-dibora-2,5-diazine, 1-amino-3-nitro-tetrahydro-1,4-dibora-2,5-diazine, 3-amino-1-nitro-tetrahydro-1,4-dibora-2,5-diazine, 1-amino-5-nitro-tetrahydro-1,4-dibora-2,5-diazine, 4-amino-2-nitro-tetrahydro-1,4-dibora-2,5-diazine, 2-amino-6-nitro-tetrahydro-1,4-dibora-2,5-diazine, 3-amino-5-nitro-tetrahydro-1,4-dibora-2,5-diazine, 1,2-dichloro-tetrahydro-1,4-dibora-2,5-diazine, 1,6-dichloro-tetrahydro-1,4-dibora-2,5-diazine, 1,2-difluoro-tetrahydro-1,4-dibora-2,5-diazine, 1,6-difluoro-tetrahydro-1,4-dibora-2,5-diazine, 2,3-difluoro-tetrahydro-1,4-dibora-2,5-diazine, 1-amino-2-nitro-tetrahydro-1,4-dibora-2,5-diazine, 1-amino-6-nitro-tetrahydro-1,4-dibora-2,5-diazine, 2-amino-1-nitro-tetrahydro-1,4-dibora-2,5-diazine, 3-amino-2-nitro-tetrahydro-1,4-dibora-2,5-diazine, 3-amino-4-nitro-tetrahydro-1,4-dibora-2,5-diazine, 1,4-dichloro-tetrahydro-1,4-dibora-2,5-diazine, 2,5-dichloro-tetrahydro-1,4-dibora-2,5-diazine, cis-3,6-dichloro-tetrahydro-1,4-dibora-2,5-diazine, trans-3,6-dichloro-tetrahydro-1,4-dibora-2,5-diazine, 1,4-difluoro-tetrahydro-1,4-dibora-2,5-diazine, 2,5-difluoro-tetrahydro-1,4-dibora-2,5-diazine, cis-3,6-difluoro-tetrahydro-1,4-dibora-2,5-diazine, trans-3,6-difluoro-tetrahydro-1,4-dibora-2,5-diazine, 2-amino-5-nitro-tetrahydro-1,4-dibora-2,5-diazine, trans-3-amino-6-nitro-tetrahydro-1,4-dibora-2,5-diazine, 3-nitro-2-amino-tetrahydro-1,4-dibora-2,5-diazine.

⁵¹IUPAC, *Nomenclature of Organic Chemistry. Sections A, B, C, D, E, F and H* (Pergamon, Oxford, 1979).

⁵²M. J. Frisch, G. W. Trucks, H. B. Schlegel *et al.*, GAUSSIAN 94, Revision B.3, Gaussian, Inc., Pittsburgh, PA, 1995.

- ⁵³ *Handbook of Chemistry and Physics*, edited by R. C. Weast, 62nd ed. (CRC Press, Boca Raton, FL, 1981).
- ⁵⁴ J. A. Pople and M. Gordon, *J. Am. Chem. Soc.* **89**, 4253 (1967).
- ⁵⁵ M. L. Olson and K. R. Sundberg, *J. Chem. Phys.* **69**, 5400 (1978).
- ⁵⁶ J. Applequist, *J. Phys. Chem.* **97**, 6016 (1993).
- ⁵⁷ L. Jensen, P.-O. Åstrand, and K. V. Mikkelsen, *Int. J. Quantum Chem.* **84**, 513 (2001).
- ⁵⁸ J. Applequist and C. O. Quicksall, *J. Chem. Phys.* **66**, 3455 (1977).
- ⁵⁹ S. F. Boys and F. Bernardi, *Mol. Phys.* **19**, 553 (1970).
- ⁶⁰ E. R. Andrew and D. Hyndman, *Discuss. Faraday Soc.* **19**, 195 (1955).
- ⁶¹ P.-O. Åstrand, A. Wallqvist, and G. Karlström, *J. Chem. Phys.* **100**, 1262 (1994).
- ⁶² P. A. Heiney, J. E. Fischer, A. R. McGhie, W. J. Romanow, A. M. Denenstein, J. P. McCauley, Jr., A. B. Smith III, and D. E. Cox, *Phys. Rev. Lett.* **66**, 2911 (1991).
- ⁶³ D. M. Bishop and M. Dupuis, *Mol. Phys.* **88**, 887 (1996).
- ⁶⁴ C. E. Dykstra and S.-Y. Liu, *J. Mol. Struct.: THEOCHEM* **135**, 357 (1986).
- ⁶⁵ J. D. Augspurger and C. E. Dykstra, *Int. J. Quantum Chem.* **43**, 135 (1992).
- ⁶⁶ M. Nakano, S. Yamada, S. Kiribayashi, and K. Yamaguchi, *Synth. Met.* **102**, 1542 (1999).
- ⁶⁷ G. Maroulis, *J. Chem. Phys.* **113**, 1813 (2000).
- ⁶⁸ J. Perez and M. Dupuis, *J. Phys. Chem.* **95**, 6525 (1991).
- ⁶⁹ S. Chen and H. A. Kurtz, *J. Mol. Struct.: THEOCHEM* **388**, 79 (1996).
- ⁷⁰ B. Kirtman, C. E. Dykstra, and B. Champagne, *Chem. Phys. Lett.* **305**, 132 (1999).
- ⁷¹ E. K. Dalskov, J. Oddershede, and D. M. Bishop, *J. Chem. Phys.* **108**, 2152 (1998).
- ⁷² R. Antoine, Ph. Dugourd, D. Rayane, E. Benichou, F. Chandezon, M. Broyer, and C. Guet, *J. Chem. Phys.* **110**, 9771 (1999).
- ⁷³ K. Ruud, D. Jonsson, and P. R. Taylor, *J. Chem. Phys.* **114**, 4331 (2001).
- ⁷⁴ W. Krättschmer, L. D. Lamb, K. Fostiropoulos, and D. R. Huffman, *Nature (London)* **347**, 354 (1990).
- ⁷⁵ A. F. Hebard, R. C. Haddon, R. M. Fleming, and A. R. Kortan, *Appl. Phys. Lett.* **59**, 2109 (1991).
- ⁷⁶ Z. H. Kafafi, J. R. Lindle, R. G. S. Pong, F. J. Bartoli, L. J. Lingg, and J. Milliken, *Chem. Phys. Lett.* **188**, 492 (1992).
- ⁷⁷ S. L. Ren, K. A. Wang, P. Zhou, Y. Wang, A. M. Rao, M. S. Meier, J. P. Selegue, and P. C. Eklund, *Appl. Phys. Lett.* **61**, 124 (1992).
- ⁷⁸ A. Ritcher and J. Sturm, *Appl. Phys. A: Mater. Sci. Process.* **61**, 163 (1995).
- ⁷⁹ P. C. Eklund, A. M. Rao, Y. Wang, K. A. Zhou, P. Wang, J. M. Holden, M. S. Dresselhaus, and G. Dresselhaus, *Thin Solid Films* **257**, 211 (1995).
- ⁸⁰ M. P. Hodges, A. J. Stone, and E. C. Lago, *J. Phys. Chem. A* **102**, 2455 (1998).
- ⁸¹ R. L. Rowley and T. Pakkanen, *J. Chem. Phys.* **110**, 3368 (1999).
- ⁸² R. L. Jaffe and G. D. Smith, *J. Chem. Phys.* **105**, 2780 (1996).
- ⁸³ See EPAPS Document No. E-JCPSA6-116-518206 for Cartesian coordinates and quantum chemical molecular polarizability tensors for the 184 aliphatic, aromatic and heterocyclic compounds used as training set. This document may be retrieved via the EPAPS homepage (<http://www.aip.org/pubservs/epaps.html>) or from <ftp.aip.org> in the directory /epaps/. See the EPAPS homepage for more information.